LINEAR DYNAMIC MODELING OF SPACECRAFT WITH VARIOUS FLEXIBLE APPENDAGES AND ON-BOARD ANGULAR MOMENTUMS

Daniel Alazard[1], **Christelle Cumer**[2], **and Khalid H.M. Tantawi**[3]

[1]*Prof. Université de Toulouse-ISAE, 10, Av. Edouard Belin, Toulouse- 31055 FRANCE. (Email: daniel.alazard@isae.fr)*
[2]*ONERA, 2, Av. Edouard Belin, Toulouse- 31055 FRANCE.*
[3]*Université de Toulouse-ISAE*

Abstract

We present here a method and some tools developed to build linear models of multi-body systems for space applications (typically satellites). The multi-body system is composed of a main body (hub) fitted with rigid and flexible appendages (solar panels, antennas, propellant tanks, ...etc) and on-board angular momentums (flywheels, control moment gyros). Each appendage can be connected to the hub by a cantilever joint or a pivot joint. More generally, our method can be applied to any open mechanical chain. In our approach, the rigid six degrees of freedom (d.o.f) (three translational and three rotational) are treated all together. That is very convenient to build linear models of complex multi-body systems. Then, the dynamics model used to design AOCS, i.e. the model between forces and torques (applied on the hub) and angular and linear position and velocity of the hub, can be derived very easily. This model can be interpreted using block diagram representation.

Key words: Modeling, Dynamics, Flexible modes, Effective mass..

INTRODUCTION

Spacecraft are very complex mechanical multi-body systems including flexible and/or rotating appendages. The design of the AOCS requires a linear model taking into account all the rigid and flexible couplings between the hub (where the AOCS acts) and the various appendages. Note that the linear assumption is quite realistic for such systems since perturbations and so motions are very small (except for very dexterous observation satellites). This linear assumption is furthermore valid in the field of future missions for deep space exploration involving formation flying of several spacecraft. For this kind of formation flying mission, it is more and more accepted that the 3 rotation d.o.f. and the 3 translation d.o.f. must be treated all together ([1]).

Therefore, a 6 d.o.f. model including couplings between rotations and translations must be developed. Lots of multi-body software are available to build such kind of models but they address the nonlinear behavior and they are too much loud to be handled at the early prototyping phase. So a tool is required to develop quickly the dynamic model and to prototype the AOCS or to analyze and to optimize the main dynamic parameters of the mechanical structure or AOCS and finally to assess the global performance of the system.

Here we propose some tools developed with MATLAB/SIMULINK to built efficiently the linear dynamic model of any open mechanical chain. More precisely, the linear multi-body model considered here is depicted on Figure 1. This model, called inverse dynamic model, gives the relationship between the inputs, which are composed of:

- the six external forces $\overrightarrow{F}_{ext}$ and torques $\overrightarrow{T}_{ext,O}$ applied on the hub (base) by the Attitude and Orbit Control System(AOCS) at a reference point O,
- the n drive torques $C_m(i)$ applied at the pivot joint i ($i = 1, \cdots, n$, n is the number of pivot joints) between an appendage and the hub,

and the output, which is composed of:

- the six linear and angular accelerations of the hub at point O (resp. $\overrightarrow{a}_O$ and $\dot{\overrightarrow{\omega}}$),
- the angular acceleration $\ddot{\theta}(i)$ of the pivot point i (for $i = 1, \cdots, n$).

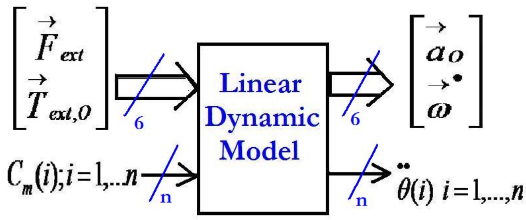

Figure 1. General inverse dynamic model

This paper introduces gradually each complexity of the modeling problem. The **first section** concerns the simplest case of two interconnected rigid bodies. Let us recall that the approach assumes that the hub (or central body or base) is rigid. In the **second section** flexible appendages are taken into account using effective mass representation. On-board angular momentum are taken into account in **section 3**. The way how a motorized pivot joint between an appendage and the hub can be taken into account is described in **section 4**. A model validation is proposed in **section 5**.

1. INTERCONNECTED RIGID BODIES MODEL

Let us consider a spacecraft composed of a rigid main body or hub (called here after the *base* B) with its center of mass at point G, and a rigid appendage A (with its center of mass C) cantilevered to the base B at point P (see Figure 4). Let us denote $R_G = (G, x, y, z)$ the reference frame rigidly attached to the hub at G and $R_P = (P, x, y, z)$ the same frame translated to point P. In the sequel the dynamic model of the appendage will be obviously given in the frame R_P.

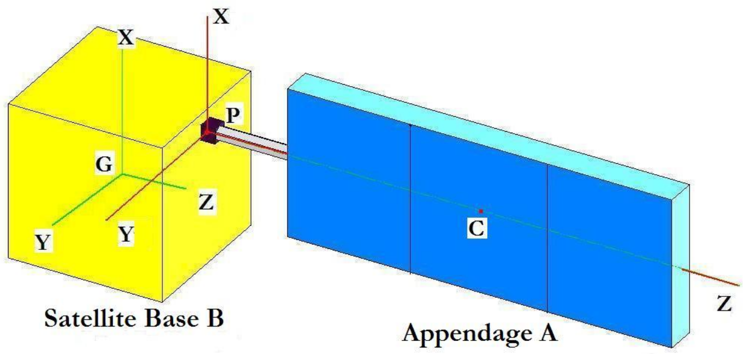

Figure 2. A simple spacecraft model, two rigid bodies connected at point P

1.1. Dynamic model of the base B at point G

Let us consider the base B alone (without appendage), according to the NEWTON's and EULER's equations, the dynamic model of the base B at its center of mass G reads as follows:

$$\begin{bmatrix} \overrightarrow{F}_{ext} \\ \overrightarrow{T}_{ext,G} \end{bmatrix} = D_G^B \begin{bmatrix} \overrightarrow{a}_G \\ \dot{\overrightarrow{\omega}} \end{bmatrix} = \begin{bmatrix} m^B I_3 & 0 \\ 0 & J_G^B \end{bmatrix} \begin{bmatrix} \overrightarrow{a}_G \\ \dot{\overrightarrow{\omega}} \end{bmatrix} \tag{1}$$

where

- m^B is the mass of the body B,
- I_n is the $n \times n$ identity matrix,
- J_G^B is the inertia matrix (in $kg.m^2$) at point G of the body B in the frame R_G,
- $\overrightarrow{\omega}$ is the absolute angular velocity vector of the body B (i.e. the angular velocity of the frame R_G or frame R_P w.r.t the inertial frame R_i in (rad/s)).
- and $\dot{\overrightarrow{\omega}} = \frac{d\overrightarrow{\omega}}{dt}|_{R_G} = \frac{d\overrightarrow{\omega}}{dt}|_{R_i}$, since $\overrightarrow{\omega}$ has the same coordinates in R_G and R_i.

In (1), the three translational accelerations and the three angular accelerations are considered together. Note that for the rotation dynamics, the relation $\overrightarrow{T}_{ext,G} = J_G^B \dot{\overrightarrow{\omega}}$ is a linear approximation, the actual non-linear dynamic equation reads:

$$\overrightarrow{T}_{ext,G} = \frac{d\overrightarrow{L}_G^B}{dt}|_{R_i} \tag{2}$$

where $\overrightarrow{L}_G^B = J_G^B \dot{\overrightarrow{\omega}}$ is the angular momentum of the base B at point G. Then, using the time-domain derivation in the body frame of base B (in which, J_G^B is constant), it comes:

$$\overrightarrow{T}_{ext,G} = J_G^B \dot{\overrightarrow{\omega}} + \overrightarrow{\omega} \times J_G^B \overrightarrow{\omega}$$

where $\times$ is the cross product.

The nonlinear term ($\overrightarrow{\omega} \times J_G^B \overrightarrow{\omega}$) on the right hand side of the equation above can be neglected if angular velocity $\overrightarrow{\omega}$ is small enough (linear assumption).

1.2. Transport of the dynamic model of B from point G to point P

Let us recall that the relation between the velocities at points P and G is :

$$\overrightarrow{V}_P = \overrightarrow{V}_G + \overrightarrow{PG} \times \overrightarrow{\omega} = \overrightarrow{V}_G + ({}^*PG)\overrightarrow{\omega} \tag{3}$$

where $({}^*PG)$ is the antisymmetric matrix associated with the vector $\overrightarrow{PG}$. That is, if $[x,\ y,\ z]_{R_c}^T$ is the coordinate vector of $\overrightarrow{GP}$ projected in any frame R_c then $({}^*GP)$ reads:

$$({}^*GP) = \begin{bmatrix} 0 & -z & y \\ z & 0 & -x \\ -y & x & 0 \end{bmatrix}_{R_c} \quad , \quad ({}^*PG) = \begin{bmatrix} 0 & z & -y \\ -z & 0 & x \\ y & -x & 0 \end{bmatrix}_{R_c} .$$

Note that equation (3) allows a vector product to be transformed into a matrix-vector product and can be projected in any frame.

Then, the six d.o.f. kinematic vectors ν_G and ν_P of the body B respectively at points G and P are given by :

$$\underbrace{\begin{bmatrix} \overrightarrow{V}_G \\ \overrightarrow{\omega} \end{bmatrix}}_{\nu_G} = \underbrace{\begin{bmatrix} I_3 & ({}^*GP) \\ 0 & I_3 \end{bmatrix}}_{\tau_{GP}} \underbrace{\begin{bmatrix} \overrightarrow{V}_P \\ \overrightarrow{\omega} \end{bmatrix}}_{\nu_P} \tag{4}$$

τ_{GP} is called the (6×6) kinematic model between the points G and P.

Now, let us consider the inertial accelerations at points P and G :

$$\overrightarrow{a}_P = \frac{d\overrightarrow{V}_P}{dt}|_{R_i} \quad \text{and} \quad \overrightarrow{a}_G = \frac{d\overrightarrow{V}_G}{dt}|_{R_i}$$

It is well-known that :

$$\overrightarrow{a}_P = \overrightarrow{a}_G + \dot{\overrightarrow{\omega}} \times \overrightarrow{GP} + \overrightarrow{\omega} \times \left(\left(\frac{d\overrightarrow{GP}}{dt} \right) |_{R_G} + \overrightarrow{\omega} \times \overrightarrow{GP} \right)$$

For a rigid body,

$$\left(\frac{d\overrightarrow{GP}}{dt} \right) |_{R_G} = 0$$

and, as explained before, all nonlinear terms can be neglected. The acceleration at point P is then deduced from the acceleration at point G by the linear relation :

$$\overrightarrow{a}_P = \overrightarrow{a}_G + ({}^*PG)\dot{\overrightarrow{\omega}} \tag{5}$$

From equation (5) one can derive the following kinematic relationship :

$$\begin{bmatrix} \overrightarrow{a}_G \\ \dot{\overrightarrow{\omega}} \end{bmatrix} = \tau_{GP} \begin{bmatrix} \overrightarrow{a}_P \\ \dot{\overrightarrow{\omega}} \end{bmatrix} = \begin{bmatrix} I_3 & ({}^*GP) \\ 0 & I_3 \end{bmatrix} \begin{bmatrix} \overrightarrow{a}_P \\ \dot{\overrightarrow{\omega}} \end{bmatrix} . \tag{6}$$

To obtain the relationship between the 6 d.o.f external force vectors at point G and at point P, it is interesting to express the external force power computed along a virtual velocity field :

$$P_{ext} = \begin{bmatrix} \overrightarrow{V}_G \\ \overrightarrow{\omega} \end{bmatrix}^T \begin{bmatrix} \overrightarrow{F}_{ext} \\ \overrightarrow{T}_{ext,G} \end{bmatrix} = \begin{bmatrix} \overrightarrow{V}_P \\ \overrightarrow{\omega} \end{bmatrix}^T \begin{bmatrix} \overrightarrow{F}_{ext} \\ \overrightarrow{T}_{ext,P} \end{bmatrix} \tag{7}$$

Combining (4) and (7), one can easily obtain :

$$\begin{bmatrix} \overrightarrow{F}_{ext} \\ \overrightarrow{T}_{ext,P} \end{bmatrix} = \tau_{GP}^T \begin{bmatrix} \overrightarrow{F}_{ext} \\ \overrightarrow{T}_{ext,G} \end{bmatrix} = \begin{bmatrix} I_3 & 0 \\ -({}^*GP) & I_3 \end{bmatrix} \begin{bmatrix} \overrightarrow{F}_{ext} \\ \overrightarrow{T}_{ext,G} \end{bmatrix} \tag{8}$$

From (6) and (8), the direct dynamic model D_P^B of the base B at point P becomes:

$$\begin{bmatrix} \overrightarrow{F}_{ext} \\ \overrightarrow{T}_{ext,P} \end{bmatrix} = \tau_{GP}^T \begin{bmatrix} m^B I_3 & 0 \\ 0 & J_G^B \end{bmatrix} \tau_{GP} \begin{bmatrix} \overrightarrow{a}_P \\ \dot{\overrightarrow{\omega}} \end{bmatrix} = D_P^B \begin{bmatrix} \overrightarrow{a}_P \\ \dot{\overrightarrow{\omega}} \end{bmatrix} \tag{9}$$

Thus the transport of the direct dynamic model of a body B from a point G to a point P reads:

$$D_P^B = \tau_{GP}^T D_G^B \tau_{GP} = \begin{bmatrix} m^B I_3 & m^B({}^*GP) \\ -m^B({}^*GP) & J_G^B - m^B({}^*GP)^2 \end{bmatrix} . \tag{10}$$

1.3. Connection with a rigid appendage

If we consider now that a rigid appendage A is cantilevered to the base B at point P, the reaction force $\overrightarrow{F}_{B/A}$ and torque $\overrightarrow{T}_{B/A,P}$ at point P between the base and the appendage must be taken into account in the dynamic model of the base. Thus equation (9) becomes:

$$\begin{bmatrix} \overrightarrow{F}_{ext} - \overrightarrow{F}_{B/A} \\ \overrightarrow{T}_{ext,P} - \overrightarrow{T}_{B/A,P} \end{bmatrix} = D_P^B \begin{bmatrix} \overrightarrow{a}_P \\ \dot{\overrightarrow{\omega}} \end{bmatrix} . \tag{11}$$

The appendage A is characterized by its own dynamic model D_P^A at point P[1]. If we assume that the only force and torque applied on the appendage A are the reaction force and torque with the base B, then one can write:

$$\begin{bmatrix} \overrightarrow{F}_{B/A} \\ \overrightarrow{T}_{B/A,P} \end{bmatrix} = D_P^A \begin{bmatrix} \overrightarrow{a}_P \\ \dot{\overrightarrow{\omega}} \end{bmatrix} \tag{12}$$

Substituting (12) in (11) we get the equation of motion of the whole system at point P:

$$\begin{aligned} \begin{bmatrix} \overrightarrow{F}_{ext} \\ \overrightarrow{T}_{ext,P} \end{bmatrix} &= (D_P^A + D_P^B) \begin{bmatrix} \overrightarrow{a}_P \\ \dot{\overrightarrow{\omega}} \end{bmatrix} \\ &= (D_P^A + \tau_{GP}^T D_G^B \tau_{GP}) \begin{bmatrix} \overrightarrow{a}_P \\ \dot{\overrightarrow{\omega}} \end{bmatrix} \end{aligned} \tag{13}$$

It could be more interesting to express the whole dynamic model at the center of mass G of the base B, since the external forces and torques will correspond to the AOCS (reaction wheel and thrust) which are mounted on the base. Then, one can directly write:

$$\begin{aligned} \begin{bmatrix} \overrightarrow{F}_{ext} \\ \overrightarrow{T}_{ext,G} \end{bmatrix} &= (\tau_{PG}^T D_P^A \tau_{PG} + D_G^B) \begin{bmatrix} \overrightarrow{a}_G \\ \dot{\overrightarrow{\omega}} \end{bmatrix} \\ &= (D_G^A + D_G^B) \begin{bmatrix} \overrightarrow{a}_G \\ \dot{\overrightarrow{\omega}} \end{bmatrix} \end{aligned} \tag{14}$$

This equation introduces the dynamic model of the appendage at the point G: (D_G^A). We can also compute the inverse dynamic model (which will be used for designing the AOCS):

$$\begin{aligned} \begin{bmatrix} \overrightarrow{a}_G \\ \dot{\overrightarrow{\omega}} \end{bmatrix} &= (D_G^B + D_G^A)^{-1} \begin{bmatrix} \overrightarrow{F}_{ext} \\ \overrightarrow{T}_{ext,G} \end{bmatrix} \\ &= (D_G^{Satellite})^{-1} \begin{bmatrix} \overrightarrow{F}_{ext} \\ \overrightarrow{T}_{ext,G} \end{bmatrix} \end{aligned} \tag{15}$$

It can be shown that:

$$(D_G^B + D_G^A)^{-1} = D_G^{B^{-1}} \left(I_6 + \tau_{PG}^T D_P^A \tau_{PG} D_G^{B^{-1}} \right)^{-1} \tag{16}$$

Equation (15) can be expressed with the block diagram presented in Figure 3 which highlights that the dynamic model of appendage acts as a feedback between acceleration and forces at point G on the base B. Such a block diagram representation will be very useful to introduce uncertainties in the various geometric or dynamic parameters.

[1] If $\overrightarrow{PC}$ is the vector between P and the center of mass C of the appendage in the frame R_P, we can also write:

$$D_P^A = \tau_{CP}^T \begin{bmatrix} m^A I_3 & 0 \\ 0 & J_C^A \end{bmatrix} \tau_{CP}$$

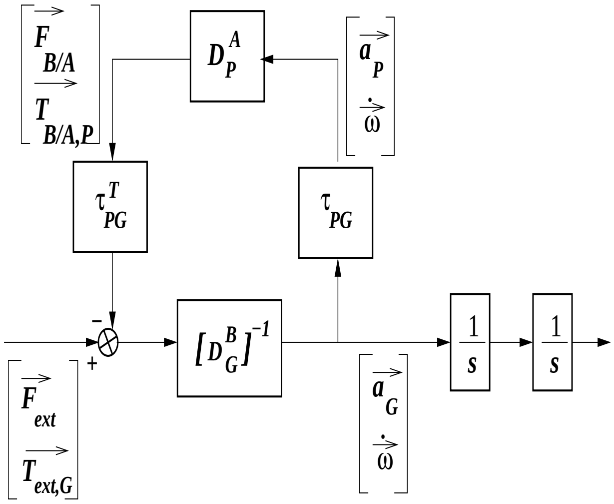

Figure 3. Block Diagram of the inverse Dynamic Model

1.4. Rigid connection with a rotation transformation

In the general case, a rotation matrix $R_{3\times3}$ between the frame $R_P^A = (P, x_P, y_P, z_P)$ (in which the dynamic model D_P^A will be described) and the frame $R_P = (P, x, y, z)$ (parallel to R_G at point P) must be taken into account. That is illustrated in Figure 4 in the special case where the appendage is rotated with an angle θ around $z - axis$, that is [2]:

$$R_{3\times3} = \begin{bmatrix} cos(\theta) & -sin(\theta) & 0 \\ sin(\theta) & cos(\theta) & 0 \\ 0 & 0 & 1 \end{bmatrix}. \tag{17}$$

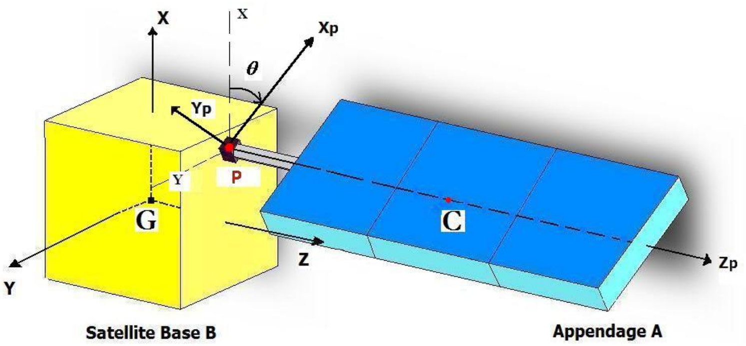

Figure 4. Rigid connection between the hub and a rotated solar array (in this figure, θ is negative).

To write the equation of motion of the whole system at point G (equation (15)), that is to compute D_G^A, we have to take into account the rotation on the dynamic model D_P^A before to transport this dynamic model from P to G:

$$D_G^A = \tau_{PG}^T \underbrace{\begin{bmatrix} R_{3\times3} & 0 \\ 0 & R_{3\times3} \end{bmatrix}}_{R_{6\times6}} D_P^A \begin{bmatrix} R_{3\times3} & 0 \\ 0 & R_{3\times3} \end{bmatrix}^T \tau_{PG} \tag{18}$$

[2] R is the coordinate matrix of R_P^A axis in R_P; that is, for any vector $\overrightarrow{v}$: $\overrightarrow{v}|_{R_P} = R\,\overrightarrow{v}|_{R_P^A}$.

2. CONNECTION OF A FLEXIBLE APPENDAGE

Flexibility of an appendage will be represented by the effective mass approach ([2]). This representation is very useful when one want to study dynamic couplings between the flexible modes of the appendage and the rigid modes of the whole system without analysis of internal deformations (or loads) of the appendage. The so called "‘Cantilever Hybrid Model"’ (see [3]) will be used: at point P, the **static** dynamic model of the appendage A (equation (12)) is now removed by the following differential equations:

$$\begin{bmatrix} \overrightarrow{F}_{B/A} \\ \overrightarrow{T}_{B/A,P} \end{bmatrix} = D_P^A \begin{bmatrix} \overrightarrow{a}_P \\ \dot{\overrightarrow{\omega}} \end{bmatrix} + L_P^T \ddot{\eta} \tag{19}$$

$$\ddot{\eta} + diag(2\xi_i w_i)\dot{\eta} + diag(w_i^2)\eta = -L_P \begin{bmatrix} \overrightarrow{a}_P \\ \dot{\overrightarrow{\omega}} \end{bmatrix} \tag{20}$$

where $L_P = [l_P^{1\,T} \quad l_P^{2\,T} \quad \cdots \quad l_P^{k\,T}]^T$.

$l^i_{P(1\times 6)}$, w_i, ξ_i are the modal contribution [3] at point P, the frequency, and the damping ratio of the flexible mode i respectively, for $i = 1, ..., k$ (k is the number of flexible modes taken into account). η is the vector of flexible modal coordinates.

The direct dynamic model of the appendage can also be described by the state-space representation:

$$\begin{bmatrix} \dot{\eta} \\ \ddot{\eta} \end{bmatrix} = \begin{bmatrix} 0_{k\times k} & I_k \\ -K_{k\times k} & -D_{k\times k} \end{bmatrix} \begin{bmatrix} \eta \\ \dot{\eta} \end{bmatrix} + \begin{bmatrix} 0_{k\times 6} \\ -L_{P_{k\times 6}} \end{bmatrix} \begin{bmatrix} \overrightarrow{a}_P \\ \dot{\overrightarrow{\omega}} \end{bmatrix}$$

$$\begin{bmatrix} \overrightarrow{F}_{B/A} \\ \overrightarrow{T}_{B/A,P} \end{bmatrix} = \begin{bmatrix} -L_P^T K & -L_P^T D \end{bmatrix} \begin{bmatrix} \eta \\ \dot{\eta} \end{bmatrix} + (D_P^A - L_P^T L_P) \begin{bmatrix} \overrightarrow{a}_P \\ \dot{\overrightarrow{\omega}} \end{bmatrix} \tag{21}$$

where $D = diag(2\xi_i w_i)$ and $K = diag(w_i^2)$.

This state-space representation allows the direct transfer matrix $M_P^A(s)$ between force and acceleration of the appendage at point P (also called **dynamic mass matrix**) to be computed:

$$\begin{bmatrix} \overrightarrow{F}_{B/A} \\ \overrightarrow{T}_{B/A,P} \end{bmatrix} = M_P^A(s) \begin{bmatrix} \overrightarrow{a}_P \\ \dot{\overrightarrow{\omega}} \end{bmatrix} \tag{22}$$

with :

$$M_P^A(s) = D_P^A - L_P^T L_P +$$
$$\begin{bmatrix} -L_P^T K & -L_P^T D \end{bmatrix}_{6\times k} \begin{bmatrix} sI_k & -I_k \\ K & (sI_k + D) \end{bmatrix}^{-1} \begin{bmatrix} 0_{k\times 6} \\ -L_{P_{k\times 6}} \end{bmatrix}.$$

In the case where flexible mode damping ratios are neglected ($D = 0$), this transfer matrix can be re-arranged in the following way:

$$M_P^A(s) = D_{P_0}^A + \sum_{i=1}^{k} D_{P_i}^A \frac{w_i^2}{s^2 + w_i^2}$$

where:

[3]if modal contribution matrix is given at point C (the appendage center of mass) and denoted L_C, then one can write: $L_P = L_C \tau_{CP}$.

- $D^A_{P_0}$ is the residual mass matrix rigidly cantilevered to the base B at point P and is given by: $D^A_{P_0} = D^A_P - L^T_P L_P = D^A_P - \sum_{i=1}^k {l^i_P}^T l^i_P$,
- $D^A_{P_i} = {l^i_P}^T l^i_P$ is rank-1 effective-mass matrix of the ith mode,
- D^A_P is the static gain (DC gain) of $M^A_P(s)$.

To build the dynamic model of the whole system (rigid base + flexible appendage), we only have to remove D^A_P by $M^A_P(s)$ (defined by state space representation (21)) in equations (13) to (16) and (18) and in the block diagram depicted in Figure 3.

3. CONNECTION WITH ON-BOARD ANGULAR MOMENTUM

In this section the appendage A is an on-board angular momentum, that is a spinning wheel. Such an on-board angular momentum can be provided by a flywheel or a CMG (Control Moment Gyro). Only the spinning wheel is considered; note that for a CMG, the gimbal joint can also be taken into account using results of section 4.

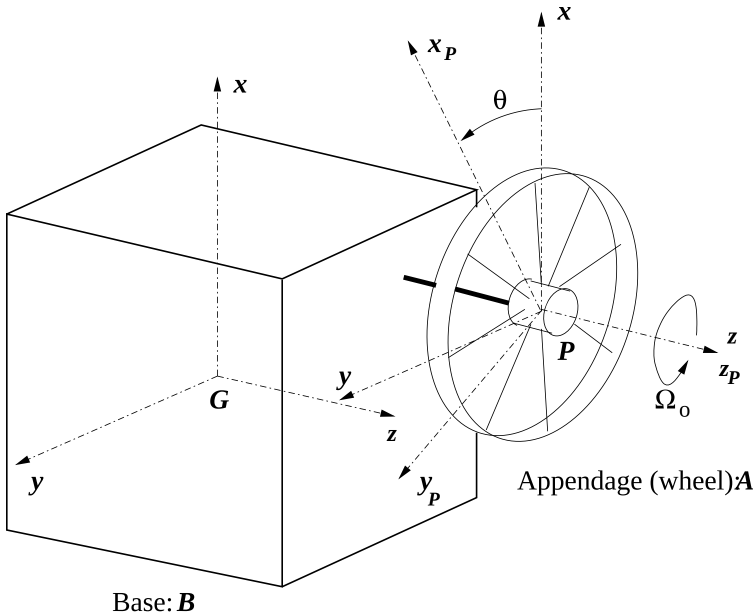

Figure 5. Connection between the hub (base B) and an onboard angular momentum.

The following assumptions will be made:

- without loss of generality, the connecting point P between the base B and the appendage A (the wheel) coincides with the center of mass C of the wheel,
- the spinning axis is along the z-axis [4] (see figure 5) and the spin rate is constant $\dot{\theta} = \Omega_0$,
- the wheel is symmetric w.r.t. $(P, \overrightarrow{z})$ axis and is statically and dynamically balanced.

Under these assumptions the dynamic model of the wheel is constant in both frames $R_P = (P, x, y, z)$ (attached to the base B) and $R^A_P = (P, x_P, y_P, z_P)$ (attached to the wheel A) and reads:

$$D^A_P = \begin{bmatrix} m^A I_3 & 0 \\ 0 & J^A_P \end{bmatrix}$$

[4] It is always possible to meet this assumption using a rotation transformation $R_{3\times 3}$ (see section 1.4)

where m^A is the mass of the wheel and $J_P^A = \begin{bmatrix} I & 0 & 0 \\ 0 & I & 0 \\ 0 & 0 & I_w \end{bmatrix}$ is the wheel inertia matrix in frame R_P or R_P^A.

The total angular momentum of the wheel w.r.t. point P reads:

$$L_P^A = J_P^A \overrightarrow{\omega} + I_w \, \dot{\theta} \, \overrightarrow{z}$$

and the fundamental principle of dynamics (using derivation in the frame R_P) provides:

$$\overrightarrow{T}_{B/A,P} = J_P^A \dot{\overrightarrow{\omega}} + I_w \, \ddot{\theta} \, \overrightarrow{z} + \overrightarrow{\omega} \times J_P^A \overrightarrow{\omega} + \overrightarrow{\omega} \times I_w \, \dot{\theta} \, \overrightarrow{z} \ ,$$

where $\dot{\overrightarrow{\omega}} = \frac{d\overrightarrow{\omega}}{dt} \, |_{R_P} = \frac{d\overrightarrow{\omega}}{dt} \, |_{R_i}$, since $\overrightarrow{\omega}$ has the same coordinates in R_P and R_i (but not in R_P^A !!).

The linearization of this equation lies on the following considerations:

- as in the previous case, the term $\overrightarrow{\omega} \times J_P^A \overrightarrow{\omega}$ can be neglected if the angular velocity $\overrightarrow{\omega}$ of the base B w.r.t inertial frame is small enough,
- $I_w \, \ddot{\theta} \, \overrightarrow{z} = \overrightarrow{0}$ as the spin rate is assumed to be constant ($\dot{\theta} = \Omega_0$). Then, the third component $T_{B/A,P_z}$ of the torque $T_{B/A,P}$ applied by the base B to the wheel A along the wheel pivot joint can represent the torque C_m applied by the wheel motor to maintain a constant spin rate Ω_0 (see section 4),
- the last term $\overrightarrow{\omega} \times I_w \, \dot{\theta} \, \overrightarrow{z}$ cannot be neglected since the spin rate $\dot{\theta} = \Omega_0$ is important.

In the frame R_P, if $[\omega_x, \ \omega_y, \ \omega_z]_{R_P}^T$ is the coordinate vector of $\overrightarrow{\omega}$, it can be easily shown that:

$$\overrightarrow{\omega} \times I_w \, \dot{\theta} \, \overrightarrow{z} = \begin{bmatrix} I_w \Omega_0 \omega_y \\ -I_w \Omega_0 \omega_x \\ 0 \end{bmatrix}_{R_P} = \begin{bmatrix} 0 & I_w \Omega_0 & 0 \\ -I_w \Omega_0 & 0 & 0 \\ 0 & 0 & 0 \end{bmatrix} \begin{bmatrix} \omega_x \\ \omega_y \\ \omega_z \end{bmatrix}_{R_P} .$$

Using intrinsic notations (already introduced in equation (3)), one can also write:

$$\overrightarrow{\omega} \times I_w \, \dot{\theta} \, \overrightarrow{z} = -I_w \Omega_0 \, ({}^*z) \, \overrightarrow{\omega}$$

where $({}^*z)$ is the antisymmetric matrix [5] associated with the spin axis $\overrightarrow{z}$. The 3×3 matrix $-I_w \Omega_0 \, ({}^*z)$ represents the **gyroscopic gain** of the wheel.

Thus, the direct angular linear model reads (using LAPLACE variable s):

$$\overrightarrow{T}_{B/A,P} = J_P^A \dot{\overrightarrow{\omega}} - I_w \Omega_0 \, ({}^*z) \, \overrightarrow{\omega} = \left(J_P^A - \frac{1}{s} I_w \Omega_0 \, ({}^*z) \right) \dot{\overrightarrow{\omega}} \ , \tag{23}$$

or considering the 6 d.o.f., the direct linear model reads:

$$\begin{bmatrix} \overrightarrow{F}_{B/A} \\ \overrightarrow{T}_{B/A,P} \end{bmatrix} = \underbrace{\left(D_P^A + \begin{bmatrix} 0_{3\times3} & 0_{3\times3} \\ 0_{3\times3} & -\frac{1}{s} I_w \Omega_0 \, ({}^*z) \end{bmatrix} \right)}_{M_P^A(s)} \begin{bmatrix} \overrightarrow{a}_P \\ \dot{\overrightarrow{\omega}} \end{bmatrix} . \tag{24}$$

To build the dynamic model of the whole system (rigid base + on-board angular momentum), we only have to remove D_P^A by $M_P^A(s)$ (defined by equation 24) in equations (13) to (16) and (18) and in the block diagram depicted in Figure 3.

Remark: If there are several on-board angular momentums connected to the hub (or the base B), then the angular rate $\overrightarrow{\omega}$ of the base (in the second member of equation (23)) is the same for each appendage (or wheel). Therefore, once the direct dynamic model of the whole system is assembled, it is possible to compute a minimal realization of this model in order

[5] In the frame R_P: $({}^*z) = \begin{bmatrix} 0 & -1 & 0 \\ 1 & 0 & 0 \\ 0 & 0 & 0 \end{bmatrix}_{R_P}$. In any frame $({}^z)$ is a rank 2 matrix; thus $M_P^A(s)$ in equation (24) is a second order system.

to remove extra integrators introduced on the angular acceleration $\dot{\vec{\omega}}$ for each appendage in equation (24). An other way to proceed is to compute the inverse dynamic model using block-diagram depicted in Figure 6 where the 6×6 gain G_P^A is defined by equation (25). But the dynamic mass matrix $M_P^A(s)$ of the appendage in equation (24) is quite useful to use results of section 4 when one wants to take into account pivot joints in appendages (CMGs for instance).

$$G_P^A = \begin{bmatrix} 0_{3\times3} & 0_{3\times3} \\ 0_{3\times3} & -I_w\Omega_0\,(^*z) \end{bmatrix} . \qquad (25)$$

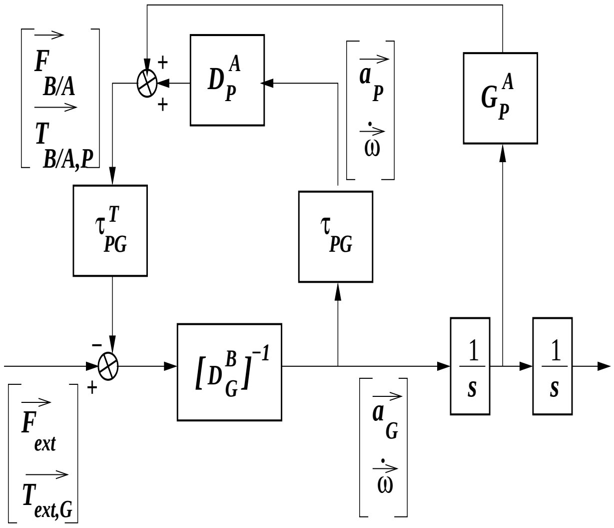

Figure 6. Block Diagram of the inverse Dynamic Model with a spinning wheel appendage.

4. PIVOT JOINT BETWEEN BASE AND APPENDAGE

In the case where the base B and the appendage A are linked by a pivot joint (around the z_P axis [6]), the reaction torque about the z_P axis is null. Then (22) projected in the frame (P, x_P, y_P, z_P) becomes:

$$\begin{bmatrix} F_{B/A_x} \\ F_{B/A_y} \\ F_{B/A_z} \\ T_{B/A,P_x} \\ T_{B/A,P_y} \\ 0 \end{bmatrix} = M_P^A(s) \begin{bmatrix} a_{P_x} \\ a_{P_y} \\ a_{P_z} \\ \dot{\omega}_x \\ \dot{\omega}_y \\ \dot{\omega}_z + \ddot{\theta} \end{bmatrix} \qquad (26)$$

where $\ddot{\theta}$ is the relative angular acceleration, along the pivot z_P-axis, of the appendage A w.r.t the base B.

If the pivot joint is motorized with a motor applying a torque C_m around z_P axis (i.e. a torque applied by the base B on the appendage A), the dynamic model of the appendage at point P becomes:

[6]It is assumed here that the pivot joint is along z_P axis in the frame R_P^A attached to the appendage. It is always possible to meet this assumption using a rotation transformation $R_{3\times3}$ (see section 1.4).

$$\begin{bmatrix} F_{B/A_x} \\ F_{B/A_y} \\ F_{B/A_z} \\ T_{B/A,P_x} \\ T_{B/A,P_y} \\ C_m \end{bmatrix} = M_P^A(s) \begin{bmatrix} a_{P_x} \\ a_{P_y} \\ a_{P_z} \\ \dot{\omega}_x \\ \dot{\omega}_y \\ \dot{\omega}_z + \ddot{\theta} \end{bmatrix} \tag{27}$$

Therefore, a new input C_m and a new output $\ddot{\theta}$ are introduced to the whole inverse dynamic model which is depicted in Figure 7 and replaces the model described by equation (15).

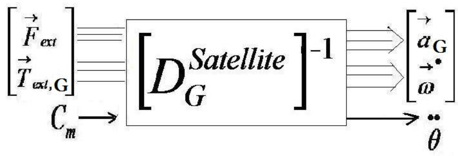

Figure 7. A schematic illustration of the inputs and outputs when pivot joints are added.

Remark: If is the appendage is an onboard angular momentum, then $M_P^A(s)$ (defined by equation (24)) depends on the spin rate which is assumed to be constant and equal to Ω_0. Thus, the result of this section are still valid only is the spin rate variation $\dot{\theta} - \Omega_0 = \int \ddot{\theta} dt$ are small enough w.r.t. the nominal spin rate Ω_0. This is the case for instance if C_m is computed to regulate the $\dot{\theta}$ around Ω_0 though a feedback gain K: $C_m = K(\Omega_0 - \dot{\theta})$. Otherwise, a new linearisation around the new spin rate must be performed.

From (27), the equation for the last row reads[7]:

$$C_m = M_P^A(s)(6, 1:5) \begin{bmatrix} a_{P_x} \\ a_{P_y} \\ a_{P_z} \\ \dot{\omega}_x \\ \dot{\omega}_y \end{bmatrix} + M_P^A(s)(6,6)\;(\dot{\omega}_z + \ddot{\theta}) \tag{28}$$

thus the pivot angular acceleration $\ddot{\theta}$ is equal to:

$$\ddot{\theta} = \frac{1}{M_P^A(s)\;(6,6)} \left[C_m - M_P^A(s)\;(6, 1:5) \begin{bmatrix} a_{P_x} \\ a_{P_y} \\ a_{P_z} \\ \dot{\omega}_x \\ \dot{\omega}_y \end{bmatrix} \right] - \dot{\omega}_z\;. \tag{29}$$

The inverse dynamic model $[D_G^{Satellite}]^{-1}$ can be described by the functional diagram depicted in Figure 8.

5. GENERALISATION AND VALIDATION

The purpose of this section is to validate the inverse dynamic model ($[D_G^{Satellite}]^{-1}$ see Figure 7) tacking into account some pivot joints between the base and some appendages by comparison with the direct dynamic model assuming that all appendages are cantilevered on the base $D_{G,cantilever}^{Satellite}$.

[7] MATLAB syntax is used to defined by $F(s)(i:j, k:l)$ the subsystem between outputs i to j and inputs k to l in the system $F(s)$.

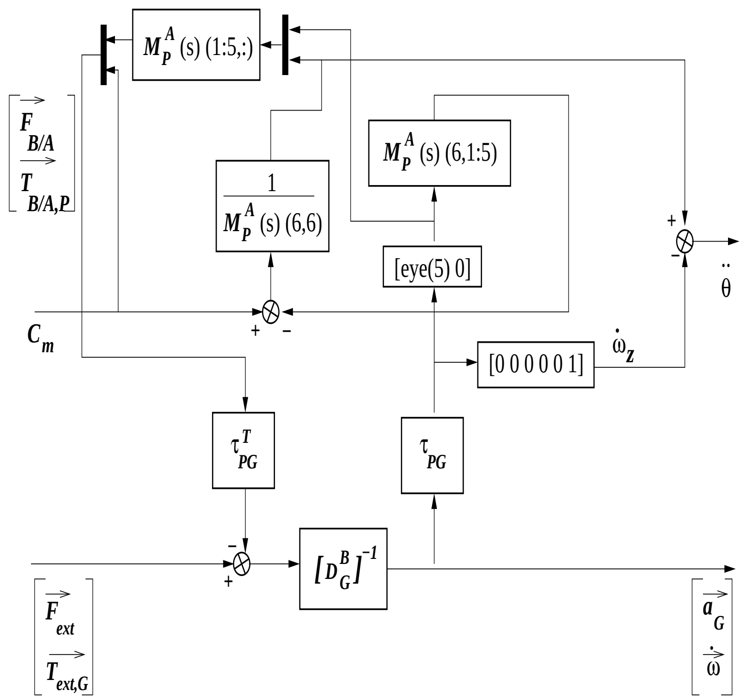

Figure 8. Block Diagram of the Inverse Dynamic Model with pivot joint

If we consider the direct model of the rigid base D_G^B and n flexible appendages A_i (defined by dynamic mass matrix $M_{P_i}^{A_i}(s)$, $i = 1, \cdots, n$) cantilevered to the base at point P_i through a rotation matrix $R_{i6\times 6}$, then using previous results of sections 1 and 2, one can compute the 6×6 direct dynamic model of the whole system:

$$D_{G,cantilever}^{Satellite} = D_G^B + \sum_{i=1}^{n} \tau_{P_iG}^T R_{i6\times 6} M_{P_i}^{A_i}(s) R_{i6\times 6}^T \tau_{P_iG} \ .$$

If we assume now that these n appendages are not cantilevered but are connected with pivot joints, then the result of section 4 allows to build the whole inverse dynamic model $[D_G^{Satellite}]^{-1}$ (see Figure 7).

This model can be detailed in the following way:

$$\begin{bmatrix} \overrightarrow{a}_G \\ \dot{\overrightarrow{\omega}} \\ \ddot{\theta}_{n\times 1} \end{bmatrix} = \begin{bmatrix} T_{11_{6\times 6}} & T_{12_{6\times n}} \\ T_{21_{n\times 6}} & T_{22_{n\times n}} \end{bmatrix} \begin{bmatrix} \overrightarrow{F}_{ext} \\ \overrightarrow{T}_{ext,G} \\ C_{m_{n\times 1}} \end{bmatrix} \tag{30}$$

T_{11} is the transfer function between $\begin{bmatrix} \overrightarrow{a}_G \\ \dot{\overrightarrow{\omega}} \end{bmatrix}$ and $\begin{bmatrix} \overrightarrow{F}_{ext} \\ \overrightarrow{T}_{ext,G} \end{bmatrix}$.

T_{12} is the transfer function between $\begin{bmatrix} \overrightarrow{a}_G \\ \dot{\overrightarrow{\omega}} \end{bmatrix}$ and $C_{m_{n\times 1}}$.

T_{21} is the transfer function between $\ddot{\theta}_{n\times 1}$ and $\begin{bmatrix} \overrightarrow{F}_{ext} \\ \overrightarrow{T}_{ext,G} \end{bmatrix}$.

T_{22} is the transfer function between $\ddot{\theta}_{n\times 1}$ and $C_{m_{n\times 1}}$.

From model $[D_G^{Satellite}]^{-1}$, one can lock pivot joints by nulling the pivot acceleration:

$$\ddot{\theta}_{n\times 1} = 0_{n\times 1}, \tag{31}$$

and then emulate cantilevered joints: indeed from equation (30) and (31) and eliminating C_m, one can derive:

$$\begin{bmatrix} \overrightarrow{a}_G \\ \dot{\overrightarrow{\omega}} \end{bmatrix}_{6\times 1} = \left[T_{11} - T_{12}T_{22}^{-1}T_{21}\right] \begin{bmatrix} \overrightarrow{F}_{ext} \\ \overrightarrow{T}_{ext,G} \end{bmatrix}_{6\times 1} . \tag{32}$$

Then one can verify that the direct dynamic model $D_{G,cantilever}^{Satellite}$ is recovered:

$$D_{G,cantilever}^{Satellite} = \left[T_{11_{6\times 6}} - T_{12_{6\times n}}T_{22_{n\times n}}^{-1}T_{21_{n\times 6}}\right]^{-1} .$$

An other way to lock pivot joints is to feedback the pivot positions to pivot torques through a very significant stiffness according to Figure 9. Then the new inverse dynamics model exhibits a high frequency flexible modes which can be reduced to provide the inverse cantilevered dynamic model.

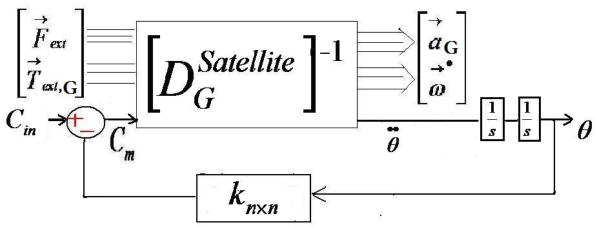

Figure 9. Pivot joints are locked using a feedback though an infinite stiffness k.

6. CONCLUSION AND PERSPECTIVES

In this paper, the linear dynamic model of a spacecraft composed of a rigid base and various flexible and rigid appendages connected to the base by a cantilever joint or a pivot joint has been developed. The build of this model lies on basic operations:

- transportation of a dynamic model to one point to an other,
- connection of 2 dynamic models,
- use of effective masses to handle dynamic mass matrix for a flexible appendage,
- use again dynamic mass matrix to take into account on-board angular momentum,
- subdivision of the dynamic mass matrix to take into account a pivot joint.

All these operations can be simply represented by a block diagram and can be performed recursively to model any kind of open mechanical chain. The reader will find in `http://personnel.supaero.fr/alazard-daniel /demos/SDT` a Matlab package called *Spacecraft Dynamics Toolbox* to develop such models and some illustrative examples (including flexible appendage or on-board angular momentum and CMGs).

The short-term perspectives of this work are the following:

- to take into account a metrological model between the accelerations at the reference point and what is measured by the sensors (linear and angular accelerometers),
- to interface our toolbox with the Linear Fractional Representation (LFR) toolbox to handle uncertain dynamic parameters in the modeling process ([4]),
- to take into account unbalances in on-board angular momentums in order to study micro-vibrations.

REFERENCES

[1] S. Gaulocher, Ch. Pittet, and J.-P. Chrétien. Six-DOF formation flying modeling and control with an application to space interferometry. In *6th International ESA Conference on Guidance, Navigation and Control Systems*, Loutraki, Greece, 17 - 20 October 2005. ESA.

[2] J.F. Imbert and A. Mamode. The effective mass concept in base motion dynamics and application to solar array dynamics. pages 343–354, Munich, Germany, 1977. Nastran User's Conference.

[3] C. Cumer and J.P. Chrétien. Minimal lft form of a spacecraft built up from two bodies. In *AIAA Guidance, Navigation, and Control Conference*. ONERA/DCSD, AIAA, 2001.

[4] J.-F. Magni. Extension of the linear fractional representation toolbox. In IEEE, editor, *Proceedings of the IEEE International Coference on CACSD*, Taipei, 2 - 4 September 2004. IEEE.

[5] R.C. Dorf and R. Bishop. *Modern Control Systems*. Prentice Hall, 2001.

[6] K. Ogata. *Modern Control Engineering*. Prentice Hall, 2002.

[7] D. Alazard and J.P. Chrétien. *Commande Active Des Structures Flexibles*. Lecture notes, SUPAERO, 2004.

[8] D.A. Wells. *Theory and Problems of Lagrangian Dynamics*. Wiley, 1993.

[9] S.C. Chapra and R. Canale. *Numerical Methods For Engineers*. McGrow Hill, 2002.